

High Gain Observer for Series-Parallel Resonant Converter

OUADIA EL MAGUIRI^{1*}, ABDELMOUNIME EL MAGRI², FARCHI ABDELMAJID¹

1IMMII-lab, University Hassan 1st, Faculty of Science and Technology, Settat

2SSDIA-lab, University of Hassan II, ENSET-M, Casablanca,

MOROCCO

* Corresponding author: Ouardia_elmaguiri@yahoo.fr

Abstract: - We are considering the problem of state observation in series-parallel resonant converters (LCC). This is a crucial issue in (LCC) output voltage control as the control model is nonlinear and involves nonphysical state variables, namely real and imaginary parts of complex electrical variables. An interconnected high gain observer is designed to get online estimates of these states. The observer is shown to be globally asymptotically stable. The global stability of the observer is analytically treated using the lyapunov theory; finally we present numerical simulation to illustrate the performance of the suggested approach.

Key-Words: - Resonant converter, Averaging approximation, state variables observation, lyapunov theory, interconnected high gain observer.

1 Introduction

In recent years, the conventional pulse-width modulated (PWM) converters are well studied and are still widely used such as power systems for computers, telephone equipment, and battery chargers. However, as mentioned in [1-3], the inefficient operation of PWM converters at very high frequencies imposes a limit on the size of reactive components of the converter and consequently on power density. In fact, the turn-on and turn-off losses caused by PWM rectangular voltage and current waveforms limit the operating frequency and produces hard switching. This yields in power losses in electrical switches and increases the potential for electromagnetic interference (EMI). To eliminate or at least mitigate the adverse effects of hard switching, most existing works have studied these converters along with circuitry arrangements to modify the current and voltage at the switches during the commutations [4-6].

Since the emergence of the resonant technology, major research efforts have been conducted to apply the enhanced features of resonant converters to practical applications. Robotics, electrostatic precipitators, X-ray power supply are a few examples in witch resonant converters are used today. These applications are treated respectively in [7], [8],[9] and [10].

The main advantages of resonant converters are well known as lower switching losses improving thus the conversion efficiency, lower electromagnetic interference; the size and weight are greatly reduced due to high operating frequency. In fact, resonant

converters can run in either the zero-current-switching (ZCS) or zero-voltage-switching (ZVS) mode. That means that turn-on or turn-off transitions of semiconductor devices can occur at zero crossings of tank voltage or current waveforms, thus reducing or eliminating some of the switching loss mechanisms. Since the losses are proportional to switching frequency, resonant converters can operate at higher switching frequencies than comparable PWM converters.

As mentioned in [11], Series and series- parallel resonant converters are variable structure systems. In fact, they are linear piecewise systems whose global behavior is strongly nonlinear. This nonlinear aspect is one of the reasons of the difficulties encountered when computing control laws, in [12], this problem is avoided by linearizing the system around a steady point and then applying the linear control techniques. An efficient method for the analysis of the series-parallel resonant converter has been proposed by [13]. There the output rectifier, filter capacitor and load are substituted by an RC load model. Unfortunately, these approaches gives only mediocre performances, to obtain a robust and high quality performances, we have to consider the nonlinearity of the circuits structure when modeling the converter, such step implies the obtention of an efficient mathematical model witch describes the dynamical behavior of the converter accurately and later, the definition of a suitable control law.

The point is that these models generally involve state variables that all are not accessible to measurement. Then, they cannot be used in control unless they allow the construction of observers.

State observation has yet to be solved for resonant converters (or was seldom been dealt with). In the present work, it is shown that such an issue can be solved for the (LCC) resonant DC/DC converter. The focus is made on the circuit of Fig 1.

Based on an extension of the first harmonic analysis proposed in [14],[15] and [16], a fifth order large signal nonlinear model that can describe the transient behavior of the converter and is useful in the development of nonlinear controllers is designed for the considered circuit. There, the output power is controlled by duty-cycle variation. However, most of involved state-variables turn out to be non-accessible to measurement. Therefore, an interconnected high gain observer is developed and shown, under mild assumptions, to be globally exponentially convergent. The global exponential convergence feature makes the proposed observer readily utilizable in the converter control. The first step in the observer design is the construction of a state diffeomorphism map leading to a transformed model that fits the required form. Using this special form, an interconnected high gain observer can be designed in a rather straight way under some global Lipschitz assumptions on the controlled part [17-19]. The gain of the proposed observer is issued from a differential Lyapunov equation.

The paper is organized as follows: mathematical modeling of the series resonant converter is addressed in Section II; theoretical design of the state observer is coped with in Section III; a global stabilities analysis of established observer is treated in section IV. The performances are illustrated by simulation in Section V; a conclusion and reference list end the paper.

2 Modeling series-parallel resonant converters

Resonant converters contain resonant L-C networks whose voltage and current waveforms vary sinusoidally during one or more subintervals of each switching period. The resonant network has the effect of filtering higher harmonic voltages such that a nearly sinusoidal current appears at the input of the resonant network [9]. Depending on how the resonant networks are combined with other circuit configurations, one can obtain several types of resonant converters. The studied series - parallel resonant DC-to-DC converter is illustrated by Fig 1.

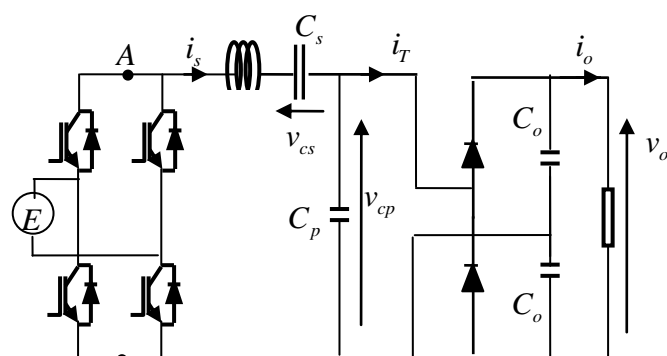


Fig 1. Series parallel resonant converter under study

A state-space representation of the system is the following:

$$L \frac{di_s}{dt} = v_{AB}(t) - v_{cs}(t) - v_{cp}(t) \quad (1)$$

$$C_s \frac{dv_{cs}}{dt} = i_s(t) \quad (2)$$

$$C_o \frac{dv_o}{dt} = abs(i_T) - \frac{2v_o}{R} \quad (3)$$

where v_{cs} and i_s denote the resonant tank voltage and current respectively; v_o is the output voltage supplying the load (here a resistor R), L and C_s designate respectively the inductance and capacitance of the series resonant tank. The parallel resonant capacitor is designed C_p . In order to simplify the analysis it will be assumed that: all the components are ideal and have no losses and that the voltage E is constant and has no ripple. The (SPRC) converter modeling is based upon the following assumptions:

Assumption 1: The voltage v_{cs} and current i_s are approximated with good accuracy by their (time varying) first harmonics

Assumption 2: The time scale of the output filter is much larger than the resonant tank so that the ripple appearing in the output voltage can be neglected and v_o can be accurately approximated by its DC-component. i.e. $v_o = V_o$.

If one observes the waveforms of Fig. 2. one can see that the resonant current i_s is almost sinusoidal. However, waveforms v_{AB} , i_T and v_{cp} do not have sinusoidal shape. That means their spectrum have high-order harmonics. Since the active power transferred to the load is dependent on the voltage v_{AB} and the resonant current i_s . As the resonant current i_s (almost) sinusoidal, i.e., only has the first harmonic component in its spectrum, the high-order

harmonics of v_{AB} will be multiplied by zero when one calculates the instantaneous power. Thus, the high-order harmonics of v_{AB} do not contribute to the power transfer to the load. For this reason, the design procedure based on the first harmonic analysis produces good results.

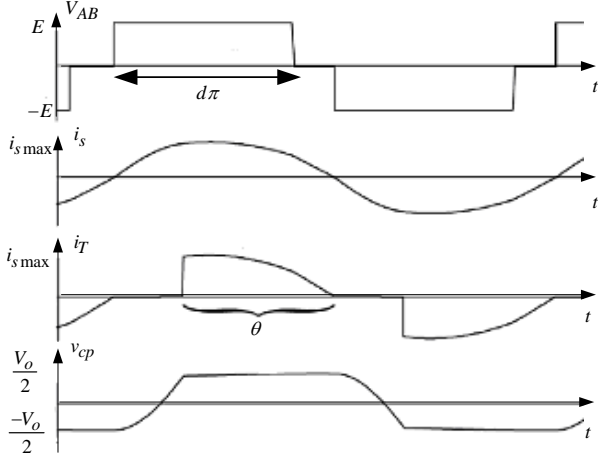


Fig 2 Time behavior of the characteristic voltages and currents

A control/observation oriented model can be obtained applying to (1-3) the first harmonic approximation procedure. This is developed in the next section.

3. First harmonic approximation

This approach relies on the assumption that the solution of a nonlinear oscillator system can be expanded in a Fourier series with time-varying coefficients. Then, a solution $x(t)$ is approximated by the Fourier series expansion of the function $\hat{x}(t, s) = x(t - T + s)$, defined in the interval $s \in [0, T]$. Mathematically, one has the following standard expressions:

$$x(t, s) = x(t - T + s) = \sum_{k=-\infty}^{+\infty} \langle x_k \rangle(t) e^{jk\omega_s(t-T+s)} \quad (4a)$$

$$\langle x_k \rangle(t) = \frac{1}{T} \int_0^T x(t - T + s) e^{-jk\omega_s(t-T+s)} ds \quad (4b)$$

with $\omega = 2\pi/T$. The coefficients $\langle x_k \rangle$ undergo the following equation:

$$\frac{d \langle x_k \rangle}{dt} = \left\langle \frac{d}{dt} x \right\rangle_k(t) - jk\omega_s \langle x_k \rangle(t) \quad (5)$$

In the case $x(t)$ is generated by a controlled nonlinear system $\dot{x} = f(x, u)$ where u denotes the control signal, it follows from (5) that:

$$\frac{d \langle x_k \rangle}{dt} = \langle f(x, u) \rangle_k(t) - jk\omega_s \langle x_k \rangle(t) \quad (6)$$

Applying (6) with $k=1$ to equations (1) to (3), we obtain the following ‘first harmonic’ equations :

$$\frac{d \langle i_s \rangle_1}{dt} = -j\omega_s \langle i_s \rangle_1 + \frac{1}{L_s} \left(-\langle v_{cs} \rangle_1 - \langle v_{cp} \rangle_1 + \langle v_{AB} \rangle_1 \right) \quad (7)$$

$$\frac{d \langle v_{cs} \rangle_1}{dt} = -j\omega_s \langle v_{cs} \rangle_1 + \frac{1}{C_s} \langle i_s \rangle_1 \quad (8)$$

$$\frac{d \langle v_o \rangle_0}{dt} = \frac{1}{C_o} \left(\langle abs(i_T) \rangle_0 - \frac{2 \langle v_o \rangle_0}{R} \right) \quad (9)$$

Given the waveforms v_{AB} and i_s shown in fig 2, the fundamental term $\langle v_{AB} \rangle_1$ is calculated as:

$$\langle v_{AB} \rangle_1 = \frac{E}{\pi} (\sin(\pi d) + j(\cos(\pi d) - 1)) \quad (10)$$

The next step is to find the Fourier representation of the term $abs(i_T)_0$, which represents the average current of the output rectifier. As shown in Fig.2, the current i_T is equal to the resonant current i_s when the voltage across the parallel capacitor is clamped to $v_o/2$ and is equal to zero otherwise. one gets

$$\begin{aligned} \langle abs(i_T) \rangle_0 &= \frac{1}{2\pi} \left(\int_{-\theta}^0 -i_{smax} \sin(\varepsilon) d\varepsilon + \int_{\pi-\theta}^{\pi} i_{smax} \sin(\varepsilon) d\varepsilon \right) \\ &= \frac{i_{smax}}{\pi} (1 - \cos \theta) \end{aligned} \quad (11)$$

where i_{smax} is the peak value of the resonant current i_s and θ is the rectifier conduction angle.

The equation of the rectifier conduction angle θ can be written as a function of state variables, inputs and circuit parameters as follows:

$$\theta = \cos^{-1} \left(\frac{\omega_s C_p V_o}{i_{smax}} - 1 \right) \quad (12)$$

From the fact that $i_{smax} = 2|\langle i_s \rangle_1|$ and $\langle v_o \rangle_0 = V_o$, equation (11) and (12) can be rewritten as

$$\langle abs(i_T) \rangle_0 = \frac{2|\langle i_s \rangle_1|}{\pi} (1 - \cos \theta) \quad (13)$$

and

$$\theta = \cos^{-1} \left(\frac{\omega_s C_p \langle v_o \rangle_0}{2 | \langle i_s \rangle_1 |} - 1 \right) \quad (14)$$

The new state variables are: $\langle i_s \rangle_1$, $\langle v_{cs} \rangle_1$ and $\langle v_o \rangle_0$. The state variables $\langle i_s \rangle_1$ and $\langle v_{cs} \rangle_1$ are complex Fourier coefficients that can be rewritten with real variables by separating the real and imaginary parts of the equations (7) and (8). Thus, the state variables can be written as:

$$\langle i_s \rangle_1 = x_1 + jx_2, \quad \langle v_{cs} \rangle_1 = x_3 + jx_4, \quad V_o = x_7 \quad (15)$$

The voltage across the parallel capacitor can be also written as a function of real variables: $\langle v_{cp} \rangle_1 = x_5 + jx_6$. x_5 and x_6 are expressed as a function of the existing state variables x_1 and x_2 by:

$$x_5 = \frac{1}{\omega_s \pi C_p} [x_1 \delta + x_2 \gamma] \quad (16)$$

$$x_6 = \frac{1}{\omega_s \pi C_p} [x_2 \delta - x_1 \gamma] \quad (17)$$

where

$$\gamma = \pi - \theta + \frac{1}{2} \sin(2\theta) \quad (18)$$

$$\delta = \sin^2(\theta) \quad (19)$$

Substituting (15) in (7)-(9) yields the following state-space representation:

$$\frac{dx_1}{dt} = \omega_s x_2 - \frac{x_3}{L} - \frac{x_5}{L} + \frac{E}{\pi L} \sin(u\pi) \quad (20)$$

$$\frac{dx_2}{dt} = -\omega_s x_1 - \frac{x_4}{L} - \frac{x_6}{L} + \frac{E}{\pi L} (\cos(u\pi) - 1) \quad (21)$$

$$\frac{dx_3}{dt} = \omega_s x_4 + \frac{x_1}{C_s} \quad (22)$$

$$\frac{dx_4}{dt} = -\omega_s x_3 + \frac{x_2}{C_s} \quad (23)$$

$$\frac{dx_7}{dt} = \frac{2\sqrt{x_1^2 + x_2^2}}{\pi C_o} (1 - \cos \theta) - \frac{2x_7}{RC_o} \quad (24)$$

where

$$x_5 = \frac{1}{\pi \omega_s C_p} [x_1 \delta + x_2 \gamma], \quad x_6 = \frac{1}{\pi \omega_s C_p} [x_2 \delta - x_1 \gamma] \quad (25)$$

$$\gamma = \pi - \theta + \frac{1}{2} \sin(2\theta); \quad \delta = \sin^2(\theta), \quad (26)$$

and

$$\theta = \cos^{-1} \left(\frac{\omega_s C_p x_7}{2\sqrt{x_1^2 + x_2^2}} - 1 \right) \quad (27)$$

where $u = d$, In the above model, the only quantities that are accessible to measurements are:

$$y_1 = x_7, \quad y_2 = \sqrt{x_1^2 + x_2^2}, \quad y_3 = \sqrt{x_3^2 + x_4^2} \quad (28)$$

That is, the variables x_1, x_2, x_3, x_4 must be estimated using some measurable quantities. To this end, an observer is built up in the next section

4 high gain observer synthesis

There is no systematic method to design an observer for a given nonlinear control system but several designs are available for nonlinear systems with specific structures. This is particularly the case for nonlinear systems that can be seen as the interconnection of several subsystems, where each subsystem satisfies specific conditions. The idea is to first design an observer for each subsystem supposing known the state of the others. Then, a global observer is developed for the whole nonlinear system combining the observers obtained separately.

4.1. Model transformation

We propose the change of coordinates $\Psi: IR^5 \rightarrow IR^6$ defined by:

$$x = \begin{pmatrix} x_1 \\ x_2 \\ x_3 \\ x_4 \\ x_7 \end{pmatrix} \rightarrow z = \Psi(x) = \begin{pmatrix} z_1 \\ z_2 \\ z_3 \\ z_4 \\ z_5 \\ z_6 \end{pmatrix} \quad (29)$$

with

$$\begin{pmatrix} z_1 = x_7 \\ z_2 = x_1 \\ z_3 = x_2 \\ z_4 = \sqrt{x_1^2 + x_2^2} \\ z_5 = x_3 \\ z_6 = x_4 \end{pmatrix} \quad (30)$$

Using (30), it follows from (20)-(24) that the new state vector z undergoes the following equations:

$$\dot{z}_1 = -\frac{2}{RC_o} z_1 + \frac{2}{\pi C_o} (1 - \cos \theta) z_4 \quad (31)$$

$$\dot{z}_2 = \omega_s z_3 - \frac{z_5}{L} - \frac{(\delta z_2 + \gamma z_3)}{\pi L \omega_s C_p} + \frac{E}{\pi L} \sin(u\pi) \quad (32)$$

$$\dot{z}_3 = -\omega_s z_2 - \frac{z_6}{L} - \frac{(\delta z_3 - \gamma z_2)}{\pi L \omega_s C_p} + \frac{E}{\pi L} (\cos u\pi - 1) \quad (33)$$

$$\begin{aligned} \dot{z}_4 = & -\frac{(z_2 z_5 + z_3 z_6)}{L z_4} - \frac{\delta}{\pi L \omega_s C_p} z_4 \\ & + \frac{E}{\pi L z_4} (\sin(\pi u) z_2 + (\cos(\pi u) - 1) z_3) \end{aligned} \quad (34)$$

$$\dot{z}_5 = \omega_s z_6 + \frac{z_2}{C_s} \quad (35)$$

$$\dot{z}_6 = -\omega_s z_5 + \frac{z_3}{C_s} \quad (36)$$

The above model can be rewritten in the form of two interconnected subsystem:

$$(\Sigma_1) \begin{cases} \dot{z}_1 = -\frac{2}{RC_o} z_1 + \frac{2}{\pi C_o} (1 - \cos \theta) z_4 \\ \dot{z}_2 = \omega_s z_3 - \frac{z_5}{L} - \frac{(\delta z_2 + \gamma z_3)}{\pi L \omega_s C_p} + \frac{E}{\pi L} \sin(u\pi) \\ \dot{z}_3 = -\omega_s z_2 - \frac{z_6}{L} - \frac{(\delta z_3 - \gamma z_2)}{\pi L \omega_s C_p} + \frac{E}{\pi L} (\cos u\pi - 1) \end{cases} \quad (37)$$

$$(\Sigma_2) \begin{cases} \dot{z}_4 = -\frac{(z_2 z_5 + z_3 z_6)}{L z_4} - \frac{\delta}{\pi L \omega_s C_p} z_4 \\ \quad + \frac{E}{\pi L z_4} (\sin(\pi u) z_2 + (\cos(\pi u) - 1) z_3) \\ \dot{z}_5 = \omega_s z_6 + \frac{z_2}{C_s} \\ \dot{z}_6 = -\omega_s z_5 + \frac{z_3}{C_s} \end{cases} \quad (38)$$

The above subsystems are given the following compact forms:

$$\begin{cases} \dot{Z}_1 = A_1(y) Z_1 + g_1(u, y, Z_2) \\ y_1 = C_1 Z_1 \end{cases} \quad (39)$$

and

$$\begin{cases} \dot{Z}_2 = A_2(y, Z_1) Z_2 + g_2(u, y, Z_1) \\ y_2 = C_2 Z_2 \end{cases} \quad (40)$$

where:

$$Z_1 = \begin{pmatrix} z_1 \\ z_2 \\ z_3 \end{pmatrix} \in \mathbb{R}^3, Z_2 = \begin{pmatrix} z_4 \\ z_5 \\ z_6 \end{pmatrix} \in \mathbb{R}^3 \quad (41)$$

$$y = [y_1 \ y_2]^T \stackrel{def}{=} [z_1 \ z_4]^T \quad (42)$$

$$A_1(y) = \begin{bmatrix} -\frac{2}{RC_o} & 0 & 0 \\ 0 & -\frac{\delta}{\pi L \omega_s C_p} & \omega_s - \frac{\gamma}{\pi L \omega_s C_p} \\ 0 & -\omega_s + \frac{\gamma}{\pi L \omega_s C_p} & -\frac{\delta}{\pi L \omega_s C_p} \end{bmatrix} \quad (43)$$

$$A_2(y, Z_1) = \begin{bmatrix} -\frac{\delta}{\pi L \omega_s C_p} & -\frac{z_2}{L z_4} & -\frac{z_3}{L z_4} \\ 0 & 0 & \omega_s \\ 0 & -\omega_s & 0 \end{bmatrix} \quad (44)$$

$$C_1 = C_2 = [1 \ 0 \ 0] \quad (45)$$

$$g_1(u, y, Z_2) = \begin{bmatrix} \frac{2}{\pi C_o} (1 - \cos \theta) z_4 \\ -\frac{z_5}{L} + \frac{E}{\pi L} \sin(u\pi) \\ -\frac{z_6}{L} + \frac{E}{\pi L} (\cos u\pi - 1) \end{bmatrix} \quad (46)$$

$$g_2(u, y, Z_1) = \begin{bmatrix} \frac{E}{\pi L z_4} (\sin(\pi u) z_2 + (\cos(\pi u) - 1) z_3) \\ \frac{z_2}{C_s} \\ \frac{z_3}{C_s} \end{bmatrix} \quad (47)$$

4.2. Observer design

In this Section, an interconnected observer will be designed for the interconnected system (39)-(40). Such design is performed under the following assumption:

Assumption 1. The signals u, y, Z_1 and Z_2 are bounded and regularly persistent to guarantee the observability of the subsystems (39) and (40), see e.g. (Besançon and Hammouri, 1998).

Under the above assumption, we propose the following observer candidate for the interconnected systems (39)-(40), see e.g.(Besançon and Hammouri, 1998):

$$\begin{cases} \dot{\hat{Z}}_1 = A_1(y) \hat{Z}_1 + g_1(u, y, \hat{Z}_2) + S_1^{-1} C_1^T (y_1 - \hat{y}_1) \\ \hat{y}_1 = C \hat{Z}_1 \end{cases} \quad (48)$$

$$\begin{cases} \dot{\hat{Z}}_2 = A_2(y, \hat{Z}_1) \hat{Z}_2 + g_2(u, y, \hat{Z}_1) + S_2^{-1} C^T (y_2 - \hat{y}_2) \\ \hat{y}_2 = C \hat{Z}_2 \end{cases} \quad (49)$$

where S_1 and S_2 are a symmetric positive definite matrix that are solution of the Lyapunov equations:

$$\dot{S}_1 = -\theta_1 S_1 - A_1^T(y) S_1 - S_1 A_1(y) + C_1^T C_1 \quad (50)$$

$$\dot{S}_2 = -\theta_2 S_2 - A_2^T(y, \hat{Z}_1) S_2 - S_2 A_2(y, \hat{Z}_1) + C_2^T C_2 \quad (51)$$

where θ_1 and θ_2 are arbitrary positive real design parameters. The other notations are defined as follows:

$$\hat{Z}_1 = [\hat{z}_1 \quad \hat{z}_2 \quad \hat{z}_3]^T, \hat{Z}_2 = [\hat{z}_4 \quad \hat{z}_5 \quad \hat{z}_6]^T \quad (52)$$

$$A_2(y, \hat{Z}_1) = \begin{bmatrix} -\frac{\delta}{\pi L \omega_s C_p} & -\frac{\hat{z}_2}{L z_4} & -\frac{\hat{z}_3}{L z_4} \\ 0 & 0 & \omega_s \\ 0 & -\omega_s & 0 \end{bmatrix} \quad (53)$$

$$g_1(u, y, \hat{Z}_2) = \begin{bmatrix} \frac{2}{\pi C_O} (1 - \cos \theta) z_4 \\ -\frac{\hat{z}_5}{L} + \frac{E}{\pi L} \sin(u\pi) \\ -\frac{\hat{z}_6}{L} + \frac{E}{\pi L} (\cos u\pi - 1) \end{bmatrix} \quad (54)$$

$$g_2(u, y, \hat{Z}_1) = \begin{bmatrix} \frac{E}{\pi L z_4} (\sin(\pi u) \hat{z}_2 + (\cos(\pi u) - 1) \hat{z}_3) \\ \frac{\hat{z}_2}{C_s} \\ \frac{\hat{z}_3}{C_s} \end{bmatrix} \quad (55)$$

The convergences of the interconnected observer defined by (48)-(49) are investigated in the next section.

5 Global stability analysis

Let us introduce the estimation errors:

$$e_1 = Z_1 - \hat{Z}_1 \quad (56)$$

$$e_2 = Z_2 - \hat{Z}_2 \quad (57)$$

It readily follows from (39), (40), (48) and (49) that the above errors undergo the following differential equations:

$$\dot{e}_1 = A_1(y)Z_1 + g_1(u, y, Z_2) - S_1^{-1}C_1^T C_1 e_1 - A_1(y)\hat{Z}_1 - g_1(u, y, \hat{Z}_2) \quad (58)$$

$$\dot{e}_2 = A_2(y, Z_1)Z_2 + g_2(u, y, Z_1) - S_2^{-1}C_2^T C_2 e_2 - A_2(y, \hat{Z}_1)\hat{Z}_2 - g_2(u, y, \hat{Z}_1) \quad (59)$$

Rearranging terms on the right sides of (58) and (59) one easily gets:

$$\dot{e}_1 = [A_1(y) - S_1^{-1}C_1^T C_1]e_1 + g_1(u, y, Z_2) - g_1(u, y, \hat{Z}_2) \quad (60)$$

$$\dot{e}_2 = [A_2(y, Z_1) - S_2^{-1}C_2^T C_2]e_2 + g_2(u, y, Z_1) - g_2(u, y, \hat{Z}_1) + [A_2(y, Z_1) - A_2(y, \hat{Z}_1)]\hat{Z}_2 \quad (61)$$

Now let consider the Lyapunov function candidate:

$$V = V_1 + V_2 \quad (62)$$

with

$$V_1(e_1) = e_1^T S_1 e_1, \quad V_2(e_2) = e_2^T S_2 e_2 \quad (63)$$

From (62) and (63), it is clear that the time-derivative of V is:

$$\dot{V} = 2e_1^T S_1 \dot{e}_1 + e_1^T \dot{S}_1 e_1 + 2e_2^T S_2 \dot{e}_2 + e_2^T \dot{S}_2 e_2 \quad (64)$$

Using (60)-(61), one obtains from (64) that:

$$\begin{aligned} \dot{V} = & e_1^T (-\theta_1 S_1 - C_1^T C_1) e_1 + e_2^T (-\theta_2 S_2 - C_2^T C_2) e_2 \\ & + 2e_2^T S_2 [A_2(y, Z_1) - A_2(y, \hat{Z}_1)] Z_2 \\ & + 2e_1^T S_1 [g_1(u, y, Z_2) - g_1(u, y, \hat{Z}_2)] \\ & + 2e_2^T S_2 [g_2(u, y, Z_1) - g_2(u, y, \hat{Z}_1)] \end{aligned} \quad (65)$$

The right side of (65) can be upper bounded as follows:

$$\begin{aligned} \dot{V} \leq & -\theta_1 e_1^T S_1 e_1 - \theta_2 e_2^T S_2 e_2 \\ & + 2\|e_2\| \|S_2\| \|A_2(y, Z_1) - A_2(y, \hat{Z}_1)\| \|Z_2\| \\ & + 2\|e_1\| \|S_1\| \|g_1(u, y, Z_2) - g_1(u, y, \hat{Z}_2)\| \\ & + 2\|e_2\| \|S_2\| \|g_2(u, y, Z_1) - g_2(u, y, \hat{Z}_1)\| \end{aligned} \quad (66)$$

Now, from the fact that $A_2(y, z_1)$ and $g_2(u, y, Z_1)$ are globally lipschitz with respect to Z_1 uniformly with respect to (u, y) . And $g_1(u, y, Z_2)$ is globally lipschitz with respect to Z_2 uniformly with respect to (u, y) we gets

$$\|A_2(y, Z_1) - A_2(y, \hat{Z}_1)\| \leq k_1 \|e_1\| \quad (67)$$

$$\|g_2(u, y, Z_1) - g_2(u, y, \hat{Z}_1)\| \leq k_2 \|e_1\| \quad (68)$$

$$\|g_1(u, y, Z_2) - g_1(u, y, \hat{Z}_2)\| \leq k_3 \|e_2\| \quad (69)$$

where k_3, k_5 and k_7 are the Lipschitz constants of the functions g_1, A_2, g_2 , respectively;

On other hand we have the following Inequalities

$$\|S_1\| \leq k_4 \quad (70)$$

$$\|S_2\| \leq k_5 \quad (71)$$

$$\|Z_1\| \leq k_6 \quad (72)$$

$$\|Z_2\| \leq k_7 \quad (73)$$

where k_4 and k_5 denote the largest eigenvalue of the positive definite matrices S_1 and S_2 , respectively; k_6 and k_7 are the upper bound of the state vectors Z_1 and Z_2 , respectively (i.e. Assumption 1).

Using (67)-(73), we get from (66) that:

$$\begin{aligned} \dot{V} \leq & -\theta_1 e_1^T S_1 e_1 - \theta_2 e_2^T S_2 e_2 \\ & + 2\mu_1 \|e_1\| \|e_2\| + 2\mu_2 \|e_1\| \|e_2\| + 2\mu_3 \|e_1\| \|e_2\| \end{aligned} \quad (74)$$

with

$$\mu_1 = k_5 k_1 k_7, \quad \mu_2 = k_1 k_3, \quad \mu_3 = k_2 k_4 \quad (75)$$

As S_1 and S_2 are bounded and positive definite, one has

$$\lambda_{\min}(S_1) \|e_1\|^2 \leq e_1^T S_1 e_1 \leq \lambda_{\max}(S_1) \|e_1\|^2 \quad (76)$$

$$\lambda_{\min}(S_2) \|e_2\|^2 \leq e_2^T S_2 e_2 \leq \lambda_{\max}(S_2) \|e_2\|^2 \quad (77)$$

where $\lambda_{\min}(S_i)$ and $\lambda_{\max}(S_i)$ are respectively the minimum and the maximum eigenvalue of S_i , $i=1,2$. In view of (76)-(77), inequality (74) implies

$$\dot{V} \leq -\theta_1 V_1 - \theta_2 V_2 + 2(\tilde{\mu}_1 + \tilde{\mu}_2 + \tilde{\mu}_3)\sqrt{V_1}\sqrt{V_2} \quad (78)$$

with

$$\tilde{\mu}_1 = \frac{\mu_1}{\sqrt{\lambda_{\min}(S_1)}\sqrt{\lambda_{\min}(S_2)}} \quad (79)$$

$$\tilde{\mu}_2 = \frac{\mu_2}{\sqrt{\lambda_{\min}(S_1)}\sqrt{\lambda_{\min}(S_2)}} \quad (80)$$

$$\tilde{\mu}_3 = \frac{\mu_3}{\sqrt{\lambda_{\min}(S_1)}\sqrt{\lambda_{\min}(S_2)}}, \quad (81)$$

Applying the well known inequality $2|ab| \leq a^2 + b^2$

with $a = \sqrt{V_1}$ and $b = \sqrt{V_2}$, one gets

$2\sqrt{V_1}\sqrt{V_2} \leq V_1 + V_2$. This, together with (78) yields:

$$\dot{V} \leq -(\theta_1 - (\tilde{\mu}_1 + \tilde{\mu}_2 + \tilde{\mu}_3))V_1 - (\theta_2 - (\tilde{\mu}_1 + \tilde{\mu}_2 + \tilde{\mu}_3))V_2 \quad (82)$$

Up to now, the design parameters θ_1 and θ_2 are arbitrary. Let them be chosen such that:

$$\theta_1 - (\tilde{\mu}_1 + \tilde{\mu}_2 + \tilde{\mu}_3) > 0 \quad (83)$$

$$\theta_2 - (\tilde{\mu}_1 + \tilde{\mu}_2 + \tilde{\mu}_3) > 0 \quad (84)$$

Then, (82) gives:

$$\dot{V} \leq -\delta V \quad (85)$$

with:

$$\delta = \min\{\theta_1 - (\tilde{\mu}_1 + \tilde{\mu}_2 + \tilde{\mu}_3), \theta_2 - (\tilde{\mu}_1 + \tilde{\mu}_2 + \tilde{\mu}_3)\} \quad (86)$$

It is readily seen from (85) that \dot{V} is negative definite, implying the global asymptotic stability of the error system (58)-(59). The result thus established is summarized in the following theorem.

Theorem 1 (main result). Consider the error system described by (58)-(59) obtained applying the interconnected observer (48) to (51) to the system (39)-(40) subject to Assumptions 1. If the observer parameters θ_1 and θ_2 are chosen as in (83)-(84), then the error system is globally exponentially stable. Consequently, the estimates \hat{Z}_1, \hat{Z}_2 will converge exponentially fast to their true values Z_1, Z_2 , whatever the initial conditions $Z_1(0), Z_2(0)$.

Remarks 1.

1) From (30) it is readily seen, that the estimates of the x_i are given by:

$$\hat{x}_1 = \hat{z}_2, \hat{x}_2 = \hat{z}_3, \hat{x}_3 = \hat{z}_5, \hat{x}_4 = \hat{z}_6$$

Then Theorem 1 implies that these estimates converge exponentially to their true values.

2) The observer (48)-(51) is a high gain type, inequality (85), together with (86), shows that the estimates convergence speed depends on the design parameters θ_1 and θ_2 : the larger these parameters, the more speedy the convergence. On the other hand, excessive values of θ_1 and θ_2 make the

observer too sensitive to output noise inherent to practical situations. Therefore, the choice of the observer parameters must be a compromise between the rapidity of estimates convergence and sensitivity of estimates to output noise.

6 Simulation results

In order to illustrate the performance of the proposed observer, digital simulations using MATLAB/SIMULINK are performed. the LCC resonant converter is given the following characteristics:

Table 1: numerical values of the LCC characteristics

parameter	Symbol	value	unit
Inductor	L	16×10^{-6}	H
Capacitor	C_s	48×10^{-6}	F
Capacitor	C_p	15×10^{-9}	F
Capacitor	C_o	1×10^{-6}	F
Resistance	R	100	Ω

The DC voltage source is fixed to $E=50V$. The initial value of the state vectors and parameter estimates are chosen as follows:

$$x(0)=[0.1 \ 0.3 \ -0.5 \ -0.2 \ 0]^T \quad (87)$$

$$\hat{Z}_1(0)=[1.5 \ 3 \ 1]^T, \hat{Z}_2(0)=[1.5 \ -3 \ -1]^T \quad (88)$$

The LCC converter is controlled in open-loop applying a variable control signal (duty-cycle). Fig (3) shows the magnitude of the complex coefficients obtained via the averaging method when the system starts up in open loop with predetermined duty cycle and switching frequency $f_s = \frac{\omega_s}{2\pi} = 256kHz$.

The results for the resonant converter, the output voltage y_1 across capacitor C_o , the resonant current y_2 and resonant voltage y_3 , are shown in Fig. 3. Fig 4 show the resulting state variables x_1, x_2, x_3, x_4 . The zoom of fig 5 illustrate the behavior of the state variables over the first 5×10^{-6} s period. Figure 6 show the state estimation errors $e_{r1} = z_1 - \hat{z}_1$; $e_{r2} = z_2 - \hat{z}_2$; $e_{r3} = z_3 - \hat{z}_3$ and $e_{r4} = z_4 - \hat{z}_4$ obtained with $\theta_1 = 200, \theta_2 = 120$. It is seen that the estimates state variables converge well to their true values within about $200\mu s$, confirming Theorem 1. This is further illustrated by the zoom of Fig. 7. Note that the convergence rate depends on the value of the observer gain.

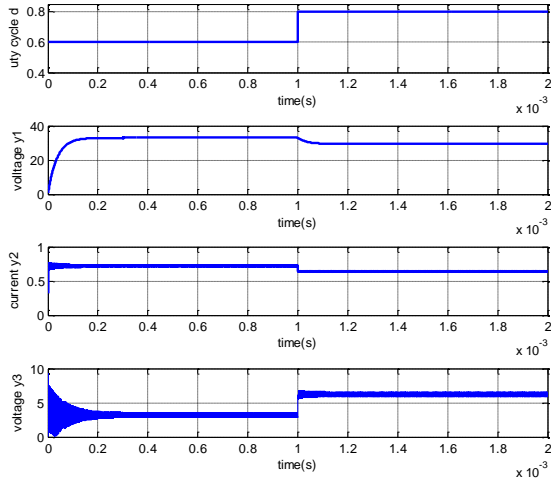


Fig 3: start up response of the amplitude of the simulated waveforms: output v_o (a) , current resonant i_s (b), resonant voltage $v_{cs}(t)$

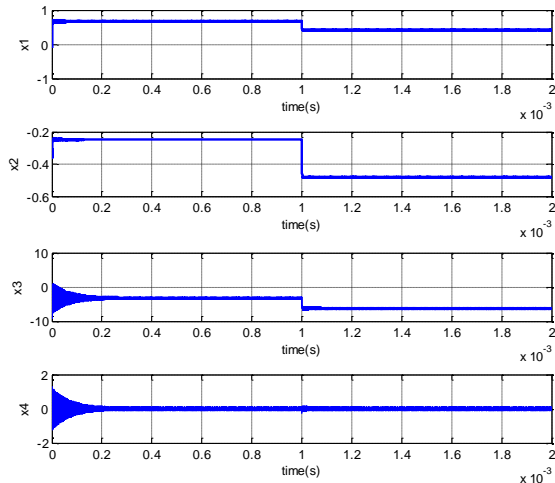


Fig 4: State variable trajectories

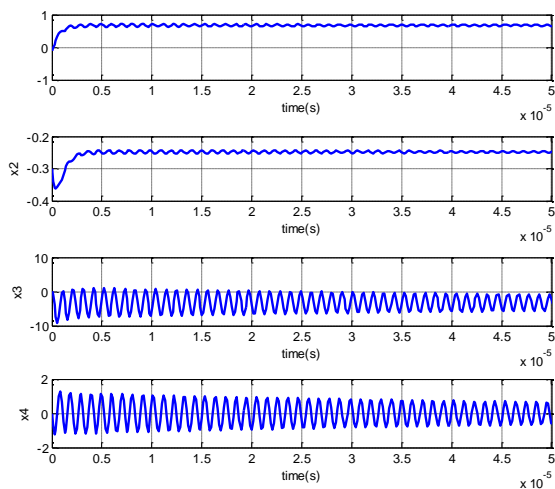


Fig 5: zoom in state variable transients

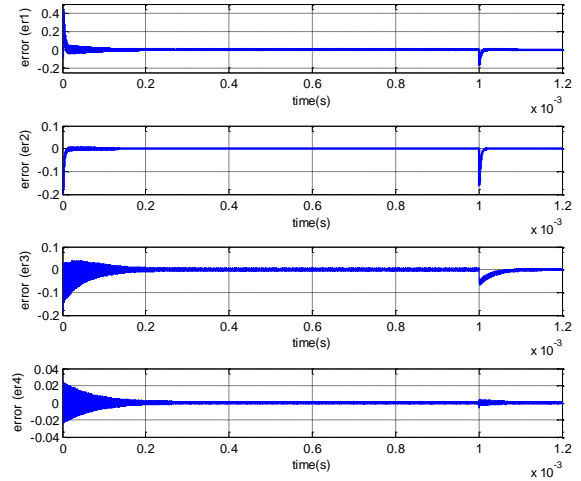


Fig 6. State estimation errors with $\theta_1 = 200, \theta_2 = 120$

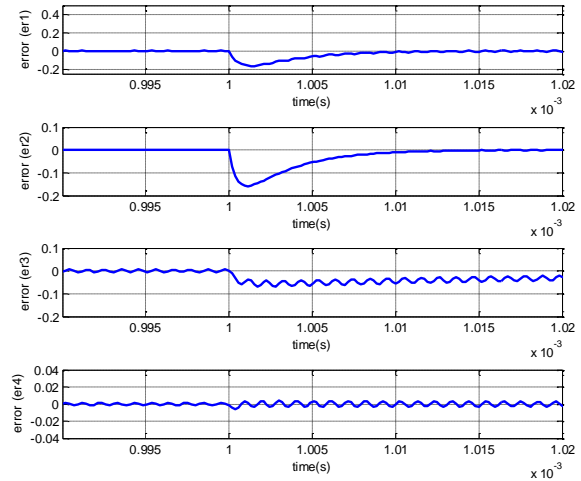


Fig 7: zoom in errors variable transients

7 Conclusion

In this paper, based on the first approximation technique, we have designed a fifth order large signal nonlinear model of the full-bridge series – parallel resonant DC-DC converter, which involves non-physical state variables. Then we have designed an interconnected high gain observer to get online estimates of these states. The observer global exponential convergence is formally established (Theorem 1). The exponential convergence feature makes the observer useful in control strategy. These results have been confirmed through numerical simulation.

REFERENCES

- [1] N.Mohan, T.M.Undeland and W.P.Robbins, 'power electronics: converters applications and Design', 3rd Ed. Hoboken, NJ: John Wiley & Sons, 2003.
- [2] I. Batarseh, 'Power Electronic Circuits' Hoboken, NJ: John Wiley & Sons, 2004.
- [3] M.K.Kazimierczuk, 'Pulse-Width Modulated DC-DC Power Converters', Chichester, UK: John Wiley & Sons, 2008.
- [4] S. Hrigua, F.Costa, C.Gautier, and B.Revol, 'New method of EMI analysis in power electronics based on semiconductors transient models: Application to SiC MOSFET/Schottky diode' in *Proc. 38th IEEE Ind. Electron. Soc. Annu. Conf. (IECON)*, 2012, pp. 590–595.
- [5] Y.Yang, D.Huang, F.C.Lee and Q.Li, 'Analysis and reduction of common mode EMI noise for resonant converters' in *Proc. 29th Annu. IEEE Appl. Power Electron. Conf. and Expo. (APEC)*, 2014, pp. 566–571.
- [6] N. Sudhakar, N.Rajasekar, V.T.Rohit, E.Rakesh, and J. Jacob, "EMI mitigation in closed loop boost converter using soft switching combined with chaotic mapping," in *Proc. Int. Conf. Advances Elect. Eng. (ICAEE)*, 2014, pp. 1–6.
- [7] O.Lucia, J.M.Burdio, I.Millan, J.Acero, and D. Puyal, 'Load adaptive control algorithm of half-bridge series resonant inverter for domestic induction heating,' *IEEE Trans. Ind. Electron.*, vol. 56, no. 8, pp. 3106–3116, Aug. 2009.
- [8] W.Li, H.Zhao, S.Li, J.Deng, T.Kan and C.C. Mi, 'Integrated LCC compensation topology for wireless charger in electric and plug-in electric vehicles,' *IEEE Trans. Ind. Electron.*, vol. 62, no. 7, pp. 4215–4225, July 2015.
- [9] Y. Wang, Y. Guan, K. Ren, W. Wang and D. Xu, 'A single-stage LED driver based on BCM boost circuit and LLC converter for street lighting system,' *IEEE Trans. Ind. Electron.*, vol. 62, no. 9, pp. 5446–5457, Sept. 2015.
- [10] Y.Tang, A. Khaligh, 'Bidirectional resonant DC–DC step-up converters for driving high-voltage actuators in mobile microrobots,' *IEEE Trans. Power Electron.*, vol.31, no.1, pp.340–352, Jan. 2016.
- [11] F.Giri, O.Elmaguiri, H. Elfadil and F.Z.Chaoui 'Nonlinear adaptive output feedback control of series resonant DC–DC converters' *Control Engineering Practice*, Vol. 19, Issue 10, PP 1238–1251, October 2011,
- [12] F.S. Cavalcante, J.W.Kolar, 'Small-Signal Model of a 5kW High-Output Voltage Capacitive-Loaded Series-Parallel Resonant DC-DC Converter'. *Proceedings of the 36th IEEE Power Electronics Specialists Conference, Recife, Brazil, June 12 - 16, pp. 1271 – 1277, 2005.*
- [13] G.Ivensky, A.Kats, S.Ben yaakov, 'A Novel RC Load Model of Parallel and Series-Parallel Resonant DC-DC Converters with Capacitive Output Filter' *IEEE Transactions on Power Electronics*, vol.14, no. 3, pp.515 – 521, May 1999
- [14] S.Sanders, J.Noworolski, X.Liu et G.Verghese 'Generalized averaging method for power conversion circuits' *IEEE PESC Record 1990*, pp.330–340
- [15] C.Olalla, I.Queinnec, R. Leyva, and A. El Aroudi, "Optimal statefeedback control of bilinear DC–DC converters with guaranteed regions of stability," *IEEE Trans. Ind. Electron.*, vol. 59, no. 10, Oct. 2012, pp. 3868–3880.
- [16] J.Linares-Flores, J.Reger, and H.Sira-Ramírez, "Load torque estimation and passivity-based control of a boost-converter/DC-motor combination," *IEEE Trans. Control Syst. Technol.*, vol. 18, no. 6, pp. 1398–1405, Nov. 2010.
- [17] G.Besançon and H.Hammouri, 'On Observer Design for Interconnected Systems', *Journal of Mathematical Systems, Estimation and Control*, Vol. 8, pp. 1–25, 1998
- [18] H.K.Khalil, and L.Praly 'high-gain observers in nonlinear feedback control' *International Journal of Robust and Nonlinear Control*, 25(6) pp,993–1015.
- [19] O.El Maguiri, F.Giri, H.Elfadil and F.Z.Chaoui, 'Interconnected state observers for series resonant converters' *IFAC Proceedings Vol 42, Issue 9, 2009, Pages 296–301*